# Adaptive MIMO Transmission for Exploiting the Capacity of Spatially Correlated Channels

Antonio Forenza, *Member, IEEE*, Matthew R. McKay, *Student Member, IEEE*, Ashish Pandharipande, *Member, IEEE*, Robert W. Heath, Jr., *Senior Member, IEEE*, and Iain B. Collings, *Senior Member, IEEE*

***Abstract*—We consider a novel low-complexity adaptive multiple-input multiple-output (MIMO) transmission technique. The approach is based on switching between low-complexity transmission schemes, including statistical beamforming, double space-time transmit diversity, and spatial multiplexing, depending on the changing channel statistics, as a practical means of approaching the spatially correlated MIMO channel capacity. We first derive new ergodic capacity expressions for each MIMO transmission scheme in spatially correlated channels. Based on these results, we demonstrate that adaptive switching between MIMO schemes yields significant capacity gains over fixed transmission schemes. We also derive accurate analytical approximations for the optimal signal-to-noise-ratio switching thresholds, which correspond to the crossing-points of the capacity curves. These thresholds are shown to vary, depending on the spatial correlation, and are used to identify key switching parameters. Finally, we propose a practical switching algorithm that is shown to yield significant spectral efficiency improvements over nonadaptive schemes for typical channel scenarios.**

***Index Terms*—Adaptive modulation, channel capacity, channel coding, fading channels, MIMO systems.**

## I. Introduction

MULTIPLE-INPUT multiple-output (MIMO) technology, through the use of multiple antennas at the transmitter and receiver sides, has been an area of intense research for its promise of increased spectral efficiency and reliability. Through the application of multiplexing and diversity techniques, MIMO technology exploits the spatial components of the wireless channel to provide capacity gain and increased link robustness. Various MIMO techniques such as beamforming (BF), spatial multiplexing (SM), and space-time coding (see [1] and references within) have been proposed to exploit the channel characteristics in different ways. The suitability and performance of a given MIMO technique depends on the channel characteristics. For instance, for line-of-sight (LOS) rank-deficient channels, or channels with high levels of spatial correlation, it is well known that robust diversity-based schemes such as BF or space-time coding should be employed. On the other hand, for rich-scattering environments SM techniques yielding high spectral efficiencies are more appropriate.

Performance tradeoffs between multiplexing and diversity have been studied in an information-theoretic sense in [2]. Practical adaptive algorithms to switch between transmit diversity (TD) and SM schemes were proposed in [3] and [4]. The algorithm described in [3] exploited the instantaneous channel knowledge to improve error rate performance for fixed data rate transmission. The adaptive method in [4] was designed to enhance spectral efficiency, exploiting statistical time/frequency selectivity indicators.

The spatial selectivity of the channel is another dimension that can be explored. Defined as in [5], the spatial selectivity depends on the characteristics of the propagation environment such as angle spread, number of scatterers, and angle of arrival/departure [6], [7]. The effect of the spatial selectivity is to create statistically uncorrelated signals across different antennas of the MIMO array, and it is typically revealed through the eigenvalues of the transmit and receive spatial correlation matrices [8]. The spatial correlation across the array elements affects the capacity [1] and error rate performance [9] of MIMO systems.

In this paper, we present a new MIMO transmission approach that adapts to the changing channel conditions based on the spatial selectivity information. The proposed system switches between different MIMO transmission schemes as a means of approaching the spatially correlated MIMO channel capacity with low-complexity. Since the adaptation is based on the long-term spatial characteristics of the channel, it can be carried out at slow rate, avoiding feedback overhead.

We consider three low-complexity open-loop MIMO schemes, namely statistical BF,[1] double space-time TD (D-STTD), and SM. We first derive new closed-form capacity results for BF, D-STTD, and SM with linear receivers and demonstrate the significant information-theoretic improve-

Manuscript received April 28, 2005; revised March 9, 2006 and April 22, 2006. The work of R. W. Heath, Jr., was supported by Freescale Semiconductor, Inc., the Office of Naval Research under Grant N00014-05-1-0169, and the National Science Foundation under Grant CCF-514194. The review of this paper was coordinated by Dr. M. Valenti.

A. Forenza is with Rearden, LLC, San Francisco, CA 94107 USA (e-mail: antonio@rearden.com).

M. R. McKay is with the Telecommunications Laboratory, School of Electrical and Information Engineering, University of Sydney, Sydney, NSW 2006 Australia, and the Information and Communication Technologies Centre, Commonwealth Scientific and Industrial Research Organisation, Epping, NSW 1710, Australia (e-mail: mckay@ee.usyd.edu.au).

A. Pandharipande is with Philips Research, 5656 AE Eindhoven, The Netherlands (e-mail: pashish@ieee.org).

R. W. Heath, Jr. is with the Wireless Networking and Communications Group, Department of Electrical and Computer Engineering, University of Texas at Austin, Austin, TX 78712 USA (e-mail: rheath@ece.utexas.edu).

I. B. Collings is with the Information and Communication Technologies Centre, Commonwealth Scientific and Industrial Research Organisation, Epping, NSW 1710, Australia (e-mail: iain.collings@csiro.au).

Color versions of one or more of the figures in this paper are available online at http://ieeexplore.ieee.org.

Digital Object Identifier 10.1109/TVT.2007.891427

[1]We define statistical BF as an open-loop scheme, under the assumption of uplink/downlink reciprocity of the channel spatial statistics.

ments obtained by adapting between these schemes based on the spatial selectivity information. We also show that the capacity of our low-complexity system approaches that of the optimal solution. We then derive accurate analytical approximations for the signal-to-noise ratios (SNRs) corresponding to the crossing-points of the BF and SM capacity curves. These crossing-points determine the relative performance of the transmission schemes and are shown to depend explicitly on the channel statistics through the eigenvalues of the spatial correlation matrices.

We finally present a practical implementation of our adaptive approach that switches between different MIMO transmission modes, with each mode comprising a particular combination of a MIMO scheme (BF/D-STTD/SM) and modulation and coding scheme. This practical system is shown to yield significant spectral efficiency improvements over nonadaptive transmission in typical channel scenarios. Preliminary results on this adaptive method have been reported in [10] and [11].

This paper is organized as follows. In Section II, we describe the wireless system under consideration and present the channel model. In Section III, we derive new closed-form capacity expressions for BF and SM, with different receivers, and the ergodic capacity for D-STTD with linear receivers. Then, in Section IV, we compute theoretical and empirical SNR thresholds to switch between different MIMO schemes. In Section V, we describe our practical adaptive MIMO transmission technique and show its performance through simulations. Finally, we draw conclusions in Section VI.

## II. System and Channel Models

We consider a narrowband MIMO system employing $N_{\mathrm{t}}$ transmit and $N_{\mathrm{r}}$ receive antennas modeled for each channel use by

$$\mathbf{y} = \sqrt{\frac{E_{\mathrm{s}}}{N_{\mathrm{t}}}}\,\mathbf{H}\mathbf{x} + \mathbf{n} \tag{1}$$

where $\mathbf{y} \in \mathbb{C}^{N_{\mathrm{r}}\times 1}$ is the receive signal vector, $\mathbf{x} \in \mathbb{C}^{N_{\mathrm{t}}\times 1}$ is the transmit signal vector subject to the power constraint $\mathcal{E}\{\|\mathbf{x}\|_2^2\} = N_{\mathrm{t}}$, $\mathbf{n} \in \mathbb{C}^{N_{\mathrm{r}}\times 1}$ is the zero-mean additive Gaussian noise vector with covariance matrix $\mathcal{E}\{\mathbf{n}\mathbf{n}^\dagger\} = N_{\mathrm{o}}\mathbf{I}_{N_{\mathrm{r}}}$, and $\mathbf{H} \in \mathbb{C}^{N_{\mathrm{r}}\times N_{\mathrm{t}}}$ is the MIMO channel matrix.[2] The SNR is defined as $\gamma_{\mathrm{o}} = E_{\mathrm{s}}/N_{\mathrm{o}}$.

We model the spatially correlated Rician MIMO channel as

$$\mathbf{H} = \sqrt{\frac{K}{K+1}}\mathbf{H}_{\ell os} + \sqrt{\frac{1}{K+1}}\mathbf{H}_{n\ell os} \tag{2}$$

where $K$ is the Rician $K$-factor, and $\mathbf{H}_{\ell os}$ and $\mathbf{H}_{n\ell os}$ are LOS and non-LOS (NLOS) components, respectively. We normalize the MIMO channel matrix such that $\mathcal{E}[\|\mathbf{H}\|_{\mathrm{F}}^2] = N_{\mathrm{r}}N_{\mathrm{t}}$. The NLOS channel matrix is given by

$$\mathbf{H}_{n\ell os} = \mathbf{R}^{1/2}\mathbf{Z}\mathbf{S}^{1/2} \tag{3}$$

where $\mathbf{Z} \in \mathbb{C}^{N_{\mathrm{r}}\times N_{\mathrm{t}}}$ contains independent complex i.i.d. Gaussian entries with zero mean and unit variance, and $\mathbf{S}$ and $\mathbf{R}$ denote the transmit and receive spatial correlation matrices, respectively, with eigenvalue decompositions

$$\mathbf{S} = \mathbf{U}_{\mathrm{s}}\mathbf{\Lambda}_{\mathrm{s}}\mathbf{U}_{\mathrm{s}}^\dagger, \quad \mathbf{R} = \mathbf{U}_{\mathrm{r}}\mathbf{\Lambda}_{\mathrm{r}}\mathbf{U}_{\mathrm{r}}^\dagger \tag{4}$$

Note that all analytical results presented in this paper apply equally to any particular spatial correlation model that can be expressed in the form (3). To make our discussion concrete, for the numerical studies we choose to consider the practical IEEE 802.11n wireless-local-area-network channel models, detailed in [12].

## III. Ergodic Capacity for Spatially Correlated MIMO Channels

In this section, we derive new analytical ergodic capacity expressions for BF, SM, and D-STTD, in spatially correlated MIMO channels. We assume that perfect channel state information is available at the receiver (CSIR) and, to facilitate BF transmission, that channel distribution information is available at the transmitter (CDIT). Although the algorithm described in Section V applies to general Rician MIMO channels, for mathematical tractability, we limit our capacity analysis to zero-mean (i.e., Rayleigh) channels. We consider channels with both single-sided (transmit side) and double-sided spatial correlation. For comparison, we first present the optimal capacity-achieving transmission strategy for the case of CDIT.

### A. Optimal Transmission

The ergodic MIMO capacity is achieved using zero-mean Gaussian input signaling and is given by the well-known formula

$$C = \max_{\mathbf{Q}:\mathrm{tr}(\mathbf{Q})=E_{\mathrm{s}}} \mathcal{E}\left[\log_2\left|\mathbf{I}_{N_{\mathrm{r}}} + \frac{\mathbf{H}\mathbf{Q}\mathbf{H}^\dagger}{N_{\mathrm{o}}}\right|\right] \tag{5}$$

where the maximization is over the set of all power-constrained input covariance matrices $\mathbf{Q}$. Under the assumptions in Section II for zero-mean spatially correlated channels, the capacity achieving $\mathbf{Q}$ is given by [13]

$$\mathbf{Q}^{\mathrm{opt}} = \mathbf{U}_{\mathrm{s}}\mathbf{\Lambda}_{\mathbf{Q}}^{\mathrm{opt}}\mathbf{U}_{\mathrm{s}}^\dagger \tag{6}$$

where $\mathbf{\Lambda}_{\mathbf{Q}}^{\mathrm{opt}}$ is the diagonal power allocation matrix

$$\mathbf{\Lambda}_{\mathbf{Q}}^{\mathrm{opt}} = \arg\max_{\mathbf{\Lambda}_{\mathbf{Q}}:\mathrm{tr}(\mathbf{\Lambda}_{\mathbf{Q}})=E_{\mathrm{s}}} \mathcal{E}\left[\log_2\left|\mathbf{I}_{N_{\mathrm{r}}} + \sum_{i=1}^{N_{\mathrm{t}}}\frac{\lambda_{s,i}\lambda_i^{\mathbf{Q}}\mathbf{w}_i\mathbf{w}_i^\dagger}{N_{\mathrm{o}}}\right|\right] \tag{7}$$

where

$$\mathbf{w}_i = \left[\sqrt{\lambda_{r,1}}w_{i,1}, \ldots, \sqrt{\lambda_{r,N_{\mathrm{r}}}}w_{i,N_{\mathrm{r}}}\right]^{\mathrm{T}} \tag{8}$$

[2] We use $\mathcal{CN}(0,1)$ to denote a random variable with real and imaginary parts that are independent identically distributed (i.i.d.) according to $\mathcal{N}(0,1/2)$, $(\cdot)^*$ to denote conjugation, $(\cdot)^{\mathrm{T}}$ to denote transposition, $(\cdot)^\dagger$ to denote conjugation and transposition, $|\cdot|$ to denote the determinant of a matrix, $\|\cdot\|_{\mathrm{F}}$ to denote the Frobenius norm, and $\mathrm{tr}(\cdot)$ to denote the trace of a matrix.

and where $w_{i,j}$ are i.i.d. complex Gaussian random variables with zero mean and unit variance. Also, $\lambda_{s,i}$, $\lambda_{r,i}$, and $\lambda_i^{\mathbf{Q}}$ denote the $i$th eigenvalue of $\mathbf{S}$, $\mathbf{R}$, and $\mathbf{Q}$, respectively. From (7) and (8), we see that the capacity achieving transmission scheme (defined by $\mathbf{Q}^{\text{opt}}$) depends explicitly on the eigenvalues of the transmit and receive correlation matrices. Unfortunately, for any given $\mathbf{S}$ and $\mathbf{R}$, the calculation of $\mathbf{\Lambda}_{\mathbf{Q}}^{\text{opt}}$ requires numerical optimization which is undesirable when designing practical systems due to its high computational complexity. The aim of the proposed adaptive method is to approximate the optimal capacity[3] by switching between low-complexity MIMO transmission schemes depending on the channel conditions.

We now present capacity expressions for the following transmission techniques: BF, SM, and D-STTD. In the next section, we compare these capacities with the optimal capacity in (5), and show that the capacity obtained by adaptively switching across these low-complexity schemes approaches the optimal capacity.

### *B. Ergodic Capacity of Statistical BF With Maximum Ratio Combining (MRC) Receiver*

In this section, we derive a new closed-form exact capacity expression for statistical BF transmission in double-sided correlated channels. We also derive a tight upper bound, which will be particularly useful for examining the relative performance of BF and SM, as shown in the next section, and for identifying switching criteria for our practical adaptive algorithm. Note that BF capacity expressions were previously derived in [14]–[16] for MISO and MIMO systems, respectively. These results, however, only considered MIMO channels with single-sided correlation.

Throughout this paper, we assume that the BF receiver employs MRC. The input covariance matrix for this system is given by

$$\mathbf{Q}^{\text{BF}} = \mathbf{U}_{\text{s}}\mathbf{\Lambda}_{\text{BF}}\mathbf{U}_{\text{s}}^{\dagger} \tag{9}$$

where

$$\mathbf{\Lambda}_{\text{BF}} = \text{diag}(E_{\text{s}}, 0, \ldots, 0). \tag{10}$$

Note that the first column of $\mathbf{U}_{\text{s}}$ is the eigenvector corresponding to the largest eigenvalue of $\mathbf{S}$, which we denote $\lambda_{s,\max}$. As mentioned in [13] and [17], statistical BF is in fact optimum (i.e., $\mathbf{\Lambda}_{\text{BF}} = \mathbf{\Lambda}_{\text{opt}}$) in the low-SNR regime.

*1) Exact Ergodic Capacity:* Using (9) and (3) in (5) gives

$$C_{\text{BF}} = \mathcal{E}\left[\log_2\left|\mathbf{I}_{N_{\text{r}}} + \frac{1}{N_{\text{o}}}\mathbf{R}^{1/2}\mathbf{Z}\mathbf{S}^{1/2}\mathbf{Q}^{\text{BF}}\mathbf{S}^{\dagger/2}\mathbf{Z}^{\dagger}\mathbf{R}^{\dagger/2}\right|\right]. \tag{11}$$

[3]For the rest of this paper, we use the term "optimal capacity" to refer to the capacity with optimum signaling in MIMO systems with only channel covariance feedback, which is given by (6) and (7).

Next, substituting the eigenvalue decompositions (4) and (9) yields

$$C_{\text{BF}} = \mathcal{E}\Bigg[\log_2\Bigg|\mathbf{I}_{N_{\text{r}}} + \frac{1}{N_{\text{o}}}\mathbf{U}_{\text{r}}\mathbf{\Lambda}_{\text{r}}^{1/2}\mathbf{U}_{\text{r}}^{\dagger}\mathbf{Z}\mathbf{U}_{\text{s}}\mathbf{\Lambda}_{\text{s}}^{1/2}\mathbf{U}_{\text{s}}^{\dagger}\mathbf{U}_{\text{s}} \times \mathbf{\Lambda}_{\text{BF}}\mathbf{U}_{\text{s}}^{\dagger}\mathbf{U}_{\text{s}}\mathbf{\Lambda}_{\text{s}}^{1/2}\mathbf{U}_{\text{s}}^{\dagger}\mathbf{Z}^{\dagger}\mathbf{U}_{\text{r}}\mathbf{\Lambda}_{\text{r}}^{1/2}\mathbf{U}_{\text{r}}^{\dagger}\Bigg|\Bigg]. \tag{12}$$

Since $\mathbf{U}_{\text{s}}$ and $\mathbf{U}_{\text{r}}$ are unitary matrices, we get $\mathbf{U}_{\text{s}}^{\dagger}\mathbf{U}_{\text{s}} = \mathbf{I}_{N_t}$, and the matrices $\mathbf{U}_{\text{r}}^{\dagger}\mathbf{Z}$ and $\mathbf{Z}\mathbf{U}_{\text{s}}$ (respectively $\mathbf{U}_{\text{s}}^{\dagger}\mathbf{Z}^{\dagger}$ and $\mathbf{Z}^{\dagger}\mathbf{U}_{\text{r}}$) have the same distribution as $\mathbf{Z}$ (respectively $\mathbf{Z}^{\dagger}$), recognizing that $\mathbf{Z}$ is invariant under unitary transformation. With these properties, the expectation in (12) is statistically equivalent to

$$C_{\text{BF}} = \mathcal{E}\left[\log_2\left|\mathbf{I}_{N_{\text{r}}} + \frac{1}{N_{\text{o}}}\mathbf{\Lambda}_{\text{r}}^{1/2}\mathbf{Z}\mathbf{\Lambda}_{\text{s}}^{1/2}\mathbf{\Lambda}_{\text{BF}}\mathbf{\Lambda}_{\text{s}}^{1/2}\mathbf{Z}^{\dagger}\mathbf{\Lambda}_{\text{r}}^{1/2}\right|\right]. \tag{13}$$

Substituting (10) into (13), we obtain

$$C_{\text{BF}} = \mathcal{E}\left[\log_2\left|\mathbf{I}_{N_{\text{r}}} + \gamma_{\text{o}}\lambda_{s,\max}\tilde{\mathbf{z}}\tilde{\mathbf{z}}^{\dagger}\right|\right] \tag{14}$$

where $\tilde{\mathbf{z}} = [\sqrt{\lambda_{r,1}}z_1, \ldots, \sqrt{\lambda_{r,N_{\text{r}}}}z_{N_{\text{r}}}]^{\text{T}}$, and the $z_i$s are i.i.d. zero-mean unit variance complex Gaussian random variables. Note that $z_i$ is the $i$th entry of the first column of $\mathbf{Z}$. We now invoke the property

$$|\mathbf{I}_n + \mathbf{A}\mathbf{B}| = |\mathbf{I}_m + \mathbf{B}\mathbf{A}| \tag{15}$$

for arbitrary $\mathbf{A} \in \mathbb{C}^{n\times m}$ and $\mathbf{B} \in \mathbb{C}^{m\times n}$ to obtain

$$C_{\text{BF}} = \mathcal{E}\left[\log_2(1 + \gamma_{\text{o}}\lambda_{s,\max}\tilde{\mathbf{z}}^{\dagger}\tilde{\mathbf{z}})\right] \tag{16}$$

$$= \mathcal{E}\left[\log_2\left(1 + \frac{\gamma_{\text{o}}\lambda_{s,\max}\eta}{2}\right)\right] \tag{17}$$

where

$$\eta = \sum_{i=1}^{N_{\text{r}}}\lambda_{r,i}\varepsilon_i \tag{18}$$

where the $\varepsilon_i$s are i.i.d. exponentially distributed random variables and, as such, $\eta$ is a central quadratic form. Since the exponential distribution is a special case of the chi-squared distributed with even (i.e., 2) degrees of freedom, we use a general result from [18] to represent the probability density function (pdf) of $\eta$ as

$$f(\eta) = \sum_{i=1}^{N_r} A_i\, p(\lambda_{r,i}\eta) \tag{19}$$

where $p(\cdot)$ denotes an exponential pdf, and

$$A_i = \left(\prod_{j=1}^{N_{\text{r}}}(-2\lambda_{r,j})^{-1}\right)\left(\prod_{j=1,j\neq i}^{N_{\text{r}}}\left(\frac{1}{2\lambda_{r,i}} - \frac{1}{2\lambda_{r,j}}\right)^{-1}\right)$$

$$= \prod_{j=1,j\neq i}^{N_{\text{r}}}\left(\frac{\lambda_{r,i}}{\lambda_{r,i} - \lambda_{r,j}}\right). \tag{20}$$

Hence, we have

$$f(\eta) = \sum_{i=1}^{N_\mathrm{r}} \prod_{j=1, j\neq i}^{N_\mathrm{r}} \left(\frac{\lambda_{r,i}}{\lambda_{r,i} - \lambda_{r,j}}\right) \frac{\exp\left(-\frac{\eta}{2\lambda_{r,i}}\right)}{2\lambda_{r,i}}. \quad (21)$$

The capacity is now given by

$$\begin{aligned} C_{\mathrm{BF}} &= \int_0^\infty \log_2\left(1 + \frac{\gamma_\mathrm{o}\lambda_{s,\max}\eta}{2}\right) f(\eta)d\eta \\ &= \sum_{i=1}^{N_\mathrm{r}} \prod_{j=1, j\neq i}^{N_\mathrm{r}} \left(\frac{\lambda_{r,i}}{\lambda_{r,i} - \lambda_{r,j}}\right) \\ &\quad \times \int_0^\infty \log_2\left(1 + \frac{\gamma_\mathrm{o}\lambda_{s,\max}\eta}{2}\right) \frac{\exp\left(-\frac{\eta}{2\lambda_{r,i}}\right)}{2\lambda_{r,i}} d\eta. \end{aligned} \quad (22)$$

To evaluate the integrals in (22), we use the property [19]

$$\int_0^\infty \ln(1+\beta x)\exp(-\mu x)dx = -\frac{1}{\mu}\exp\left(\frac{\mu}{\beta}\right)\mathrm{Ei}\left(-\frac{\mu}{\beta}\right) \quad (23)$$

for $\mathrm{Re}(\mu) > 0$ and $-\pi < \arg\beta < \pi$, where $\mathrm{Ei}(\cdot)$ is the exponential integral. For Hermitian positive definite $\mathbf{R}$, the required conditions are met, and we use (23) to obtain

$$\begin{aligned} C_{\mathrm{BF}} = -\frac{1}{\ln 2}\sum_{i=1}^{N_\mathrm{r}} \Bigg( &\prod_{j=1, j\neq i}^{N_\mathrm{r}} \left(\frac{\lambda_{r,i}}{\lambda_{r,i} - \lambda_{r,j}}\right) \\ &\times \exp\left(\frac{1}{\gamma_\mathrm{o}\lambda_{s,\max}\lambda_{r,i}}\right) \mathrm{Ei}\left(-\frac{1}{\gamma_\mathrm{o}\lambda_{s,\max}\lambda_{r,i}}\right)\Bigg). \end{aligned} \quad (24)$$

We clearly see that the BF capacity depends explicitly on the long-term channel characteristics through the eigenvalues of the spatial correlation matrices.

*2) Ergodic Capacity Upper Bound:* We upper bound the BF capacity by applying Jensen's inequality to (16) as follows:

$$\begin{aligned} C_{\mathrm{BF}} &= \mathcal{E}\left[\log_2(1 + \gamma_\mathrm{o}\lambda_{s,\max}\tilde{\mathbf{z}}^\dagger\tilde{\mathbf{z}})\right] & (25)\\ &\leq \log_2\left(1 + \gamma_\mathrm{o}\lambda_{s,\max}\mathcal{E}[\tilde{\mathbf{z}}^\dagger\tilde{\mathbf{z}}]\right) & (26)\\ &= \log_2(1 + \gamma_\mathrm{o}\lambda_{s,\max}N_\mathrm{r}). & (27) \end{aligned}$$

Note that this upper bound applies for both single-sided and double-sided correlated Rayleigh MIMO channels.

*3) Numerical Capacity Results:* In Fig. 1, we present BF capacity curves based on the exact expression (24) and upper bound (27). The correlated MIMO channels are generated according to IEEE 802.11n model D (NLOS) in [12]. For comparison, empirically generated BF capacity curves, obtained using (5), are also shown. We clearly see that, in all cases, the exact capacity curves match precisely with the empirical results, and the upper bound is tight.

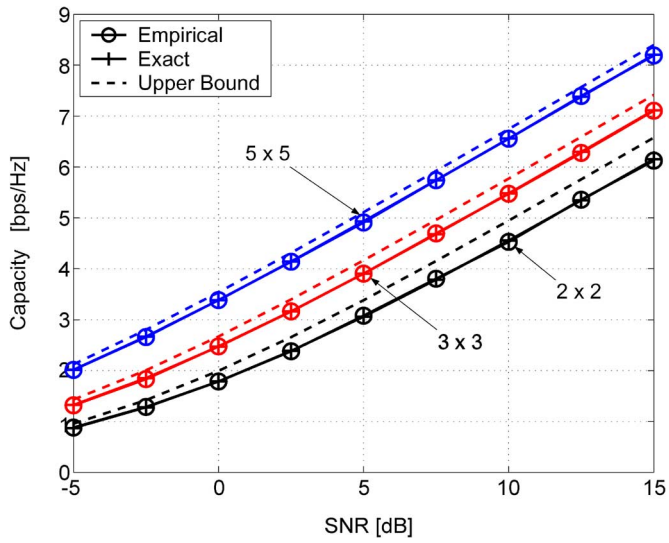


Fig. 1. Empirical, exact, and upper bound to the ergodic capacity of BF, in double-sided correlated channel model D (NLOS), with different antenna configurations ($N_\mathrm{t} \times N_\mathrm{r}$).

### C. Ergodic Capacity of Spatial Multiplexing (SM) With Linear Receivers

In this section, we derive a new closed-form exact capacity expression for SM with linear receivers. As for the BF case, we also derive a tight upper bound which will be useful for examining the relative performance of BF and SM in the next section and for identifying switching criteria for our practical algorithm.

For SM transmission, we assume equal-power allocation across the $N_\mathrm{t}$ transmit antennas, such that the input covariance matrix is given by

$$\mathbf{Q}^{\mathrm{SM}} = \frac{E_\mathrm{s}}{N_\mathrm{t}}\mathbf{I}_{N_\mathrm{t}}. \quad (28)$$

In this case, the SM capacity has been investigated in the literature when high-complexity maximum-likelihood (ML) receivers are employed. In particular, exact expressions and tight bounds are now available for both single-sided [20], [21] and double-sided [22] correlated Rayleigh MIMO channels. Recently, in [23] and [24], capacity bounds were also derived for SM with ML receivers, for the more general case of double-sided correlated Rician MIMO channels. In [25], it was shown that, for systems with $N_\mathrm{t} \leq N_\mathrm{r}$, SM transmission with ML receivers is in fact optimum (i.e., $\mathbf{Q}^{\mathrm{SM}} = \mathbf{Q}^{\mathrm{opt}}$) in the high-SNR regime.

In contrast, closed-form capacity results for SM systems employing low-complexity linear receivers do not appear to be available.

*1) Exact Ergodic Capacity:* For SM with linear receivers, the MIMO channel is effectively decoupled into $N_\mathrm{t}$ parallel streams, for which the capacity is given by [26]

$$C_{\mathrm{SM}} = \sum_{k=1}^{N_t} \mathcal{E}_{\gamma_k}\left[\log_2(1 + \gamma_k)\right] \quad (29)$$

where $\gamma_k$ is the conditional postprocessing SNR for the $k$th stream. We consider minimum mean-square error (mmse) and zero-forcing (ZF) linear receivers, for which $\gamma_k$ is given by

$$\gamma_k = \frac{1}{\left[\left(\mathbf{I}_{N_t} + \frac{\gamma_o}{N_t}\mathbf{H}^\dagger\mathbf{H}\right)^{-1}\right]_{k,k}} - 1 \tag{30}$$

and

$$\gamma_k = \frac{\gamma_o}{N_t}\frac{1}{[(\mathbf{H}^\dagger\mathbf{H})^{-1}]_{k,k}} \tag{31}$$

respectively [27], where $[\cdot]_{k,k}$ denotes the $k$th diagonal element.

The expectations in (29) cannot be computed in closed-form in general. To make our analysis mathematically tractable, for the remainder of this section, we consider transmit correlated Rayleigh MIMO channels (i.e., $\mathbf{R} = \mathbf{I}_{N_r}$) and ZF receivers.[4] Note, however, that MMSE receivers slightly outperform ZF receivers at low to moderate SNRs, and hence these receivers will be considered for our practical adaptive system proposed in Section V. For the ZF case with transmit correlation, $\gamma_k$ has pdf [26]

$$f(\gamma_k) = \frac{N_t[\mathbf{S}^{-1}]_{k,k}}{\gamma_o}\frac{\exp\left(-\frac{\gamma_k N_t[\mathbf{S}^{-1}]_{k,k}}{\gamma_o}\right)}{\Gamma(N_r - N_t + 1)} \times \left(\frac{\gamma_k N_t[\mathbf{S}^{-1}]_{k,k}}{\gamma_o}\right)^{N_r - N_t}. \tag{32}$$

Using (32), along with the identity [15]

$$\int_0^\infty \ln(1+ay)y^{n-1}\exp(-cy)dy = \Gamma(n)\exp\left(\frac{c}{a}\right)\sum_{m=1}^{n}\frac{\Gamma\left(-n+m,\frac{c}{a}\right)}{c^m a^{n-m}} \tag{33}$$

where $\Gamma(\cdot,\cdot)$ is the incomplete gamma function, and the relation [28]

$$[\mathbf{S}^{-1}]_{k,k} = \frac{|\mathbf{S}^{kk}|}{|\mathbf{S}|} \tag{34}$$

where $\mathbf{S}^{kk}$ corresponds to $\mathbf{S}$ with the $k$th row and column removed, the SM capacity (29) can be evaluated as

$$C_{SM} = \sum_{k=1}^{N_t}\frac{\exp\left(\frac{|\mathbf{S}^{kk}|N_t}{|\mathbf{S}|\gamma_o}\right)}{\ln 2} \times \sum_{m=1}^{N_r - N_t + 1}\frac{\Gamma\left(m - N_r + N_t - 1, \frac{|\mathbf{S}^{kk}|N_t}{|\mathbf{S}|\gamma_o}\right)}{\left(\frac{|\mathbf{S}^{kk}|N_t}{|\mathbf{S}|\gamma_o}\right)^{m - N_r + N_t - 1}}. \tag{35}$$

[4]Note that the results also apply for channels with receive correlation when $N_r = N_t$. In this case, $\mathbf{S}$ is replaced by $\mathbf{R}$ in the final expression.

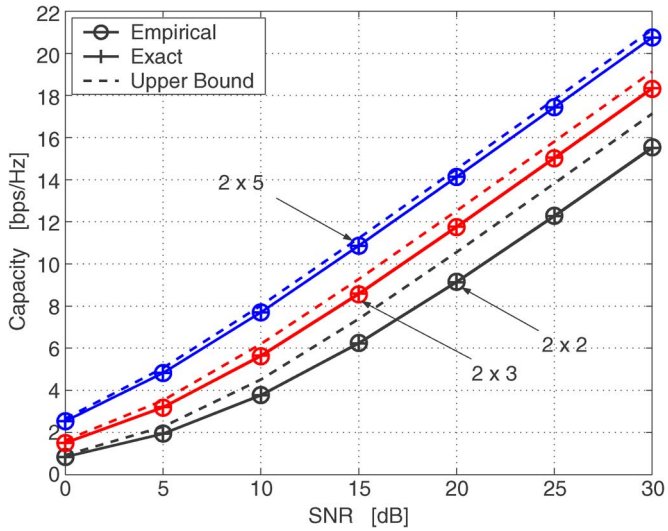


Fig. 2. Empirical, exact and upper bound to the ergodic capacity of $(2 \times N_r)$ SM system with ZF receiver, in single-sided correlated channel model D (NLOS).

As for the BF case, we see that the SM capacity depends on the long-term channel characteristics through the eigenvalues of the spatial correlation matrix (i.e., through the determinant).

This dependence is exploited by our practical adaptive algorithm presented in Section V.

*2) Ergodic Capacity Upper Bound:* We upper bound the capacity of SM with ZF receivers by applying Jensen's inequality to (29) as follows:

$$C_{SM} = \sum_{k=1}^{N_t}\mathcal{E}_{\gamma_k}\left[\log_2(1+\gamma_k)\right] \le \sum_{k=1}^{N_t}\log_2\left(1+\mathcal{E}_{\gamma_k}[\gamma_k]\right). \tag{36}$$

We evaluate the expectations in (36) using the pdf of $\gamma_k$ given in (32), and the identity [19]

$$\int_0^\infty x^n\exp(-\mu x)dx = n!\mu^{-n-1} \tag{37}$$

for $\Re e[\mu] > 0$ and simplify the resulting expression to obtain the capacity upper bound

$$C_{SM} \le \sum_{k=1}^{N_t}\log_2\left(1 + \frac{(N_r - N_t + 1)|\mathbf{S}|\gamma_o}{N_t|\mathbf{S}^{kk}|}\right). \tag{38}$$

*3) Numerical Capacity Results:* Fig. 2 compares the exact capacity (35) and upper bound (38) for SM with ZF receivers against the empirical results obtained from Monte Carlo simulations. As for the BF case, we generated the MIMO channel according to model D (NLOS) in [12], with single-sided correlation and different antenna configurations. Fig. 2 shows perfect

match between the exact and empirical capacity and the upper bound is relatively tight, especially for high numbers of receive antennas.

### D. Ergodic Capacity of D-STTD With Linear Receivers

In this section, we consider the capacity of D-STTD. Although closed-form solutions are difficult to obtain even for the simplest case of i.i.d. Rayleigh MIMO channels (see next page), here, we formulate a new capacity expression suitable for efficient numerical evaluation.

Consider the D-STTD scheme proposed in [29], where $N_{\mathrm{t}} = 4$ transmitted symbols (denoted $x_1, \ldots, x_4$ in the following) are encoded over two consecutive channel uses. Following the notations in [29], we define the stacked signal vectors

$$\bar{\mathbf{y}} \triangleq \begin{bmatrix} \bar{\mathbf{y}}_1 \\ \bar{\mathbf{y}}_2 \\ \vdots \\ \bar{\mathbf{y}}_{N_{\mathrm{r}}} \end{bmatrix}, \bar{\mathbf{x}} \triangleq \begin{bmatrix} x_1 \\ x_2^* \\ x_3 \\ x_4^* \end{bmatrix}, \mathcal{H} \triangleq \begin{bmatrix} \mathcal{H}_{1,a} & \mathcal{H}_{1,b} \\ \mathcal{H}_{2,a} & \mathcal{H}_{2,b} \\ \vdots & \vdots \\ \mathcal{H}_{N_{\mathrm{r}},a} & \mathcal{H}_{N_{\mathrm{r}},b} \end{bmatrix} \tag{39}$$

with $\bar{\mathbf{y}}_m = [y_m(0), y_m^*(1)]^{\mathrm{T}}$ and

$$\mathcal{H}_{m,a} \triangleq \begin{bmatrix} h_{m,1} & -h_{m,2} \\ h_{m,2}^* & h_{m,1}^* \end{bmatrix}, \mathcal{H}_{m,b} \triangleq \begin{bmatrix} h_{m,3} & -h_{m,4} \\ h_{m,4}^* & h_{m,3}^* \end{bmatrix} \tag{40}$$

where $h_{i,j}$ denotes the $(i,j)$th entry of the MIMO channel matrix $\mathbf{H}$ in (1). The equivalent input-output relation for D-STTD transmission can then be written as

$$\bar{\mathbf{y}} = \sqrt{\frac{E_{\mathrm{s}}}{N_{\mathrm{t}}}} \mathcal{H} \bar{\mathbf{x}} + \bar{\mathbf{n}} \tag{41}$$

where $\bar{\mathbf{n}}$ is the complex Gaussian noise. Note that the elements $\bar{\mathbf{y}}_m$ of the equivalent received vector $\bar{\mathbf{y}}$ contain the signals at the $m$th receive antenna over the two consecutive symbol time-slots.

As for SM, we consider low-complexity linear receivers. The postprocessing SNR for the $k$th stream (i.e., $\gamma_k$) in this case is then given by (30) and (31) for mmse and ZF receivers, respectively, but with $\mathbf{H}$ replaced by the equivalent D-STTD channel matrix $\mathcal{H}$ in (39).

The D-STTD capacity with linear receivers can be derived based on an approach similar to [30] (where linear-dispersion codes were considered) and has the expression

$$C_{\text{D-STTD}} = \mathcal{E}_{\gamma_k} \left[ \frac{1}{2} \sum_{k=1}^{N_{\mathrm{t}}} \log_2(1 + \gamma_k) \right] \tag{42}$$

where the normalization factor of $1/2$ accounts for the two channel uses spanned by the D-STTD symbols. To evaluate (42), we require a closed-form expression for the pdf of $\gamma_k$. Such an expression cannot be obtained even in the simplest i.i.d. Rayleigh case since $\mathcal{H}\mathcal{H}^{\dagger}$ does not follow a complex Wishart distribution. However, the computation of (42) can be made efficient by observing that $\gamma_1 = \gamma_2$ and $\gamma_3 = \gamma_4$ and, moreover, that the random variables $\gamma_k$ (for $k = 1, \ldots, 4$) are identically distributed (see the Appendix for proof). As such, (42) can be simplified as[5]

$$C_{\text{D-STTD}} = 2\, \mathcal{E}_{\gamma} \left[ \log_2(1 + \gamma) \right]. \tag{43}$$

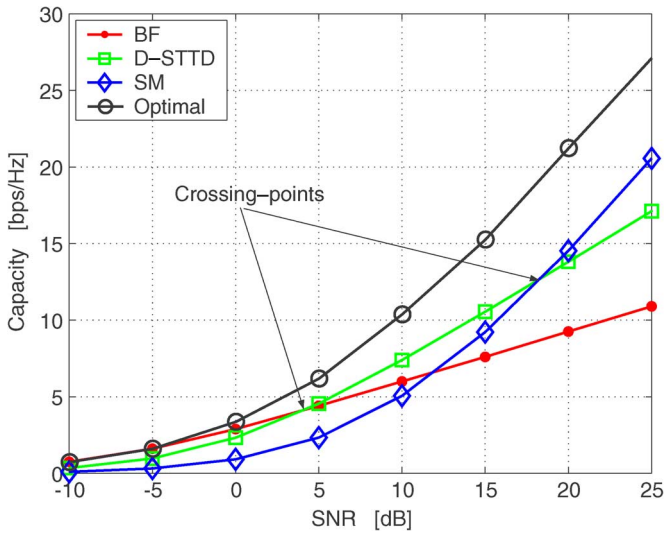


Fig. 3. Mean capacity for BF, D-STTD (with ZF), SM (with ZF), and optimal transmission in the IEEE 802.11n channel model F (NLOS).

## IV. Relative Capacity Investigation

In this section, we invoke the results of the preceding section to investigate the relative capacity performance of the BF, D-STTD, and SM schemes in spatially correlated Rayleigh MIMO channels.

### A. Comparison of BF, D-STTD, and SM Ergodic Capacities

In Fig. 3, we present ergodic capacity curves for BF, D-STTD with ZF receivers, and SM with ZF receivers, based on (24), (43), and (29), respectively. Results are shown for a $4 \times 4$ MIMO system, and the channel is generated according to IEEE 802.11n channel model F (NLOS) [12]. The optimal capacity curve is also shown for comparison, which were generated by numerically solving the optimization problem (7). Note that, since the objective function in (7) is not convex, and because the problem is subject to an equality constraint, the maximization in (7) was performed using a constrained genetic algorithm [31].

As marked on the figure, we see that the capacity curves for the three low-complexity schemes intersect, and that each scheme provides the highest capacity, with respect to the others, for a certain range of SNRs. Specifically, we see that at low-SNRs, BF achieves the highest capacity of the low-complexity schemes. In fact, for SNRs below $-5$ dB, BF achieves the optimal capacity, which agrees with previous results in [13], [17]. For moderate SNRs (i.e., between 4 and 18 dB), D-STTD achieves the highest capacity, whereas SM performs the best for high SNRs. We note that the capacity gap at

[5]Note that we drop the $k$ subscript since the SNR statistics are identical for each stream.

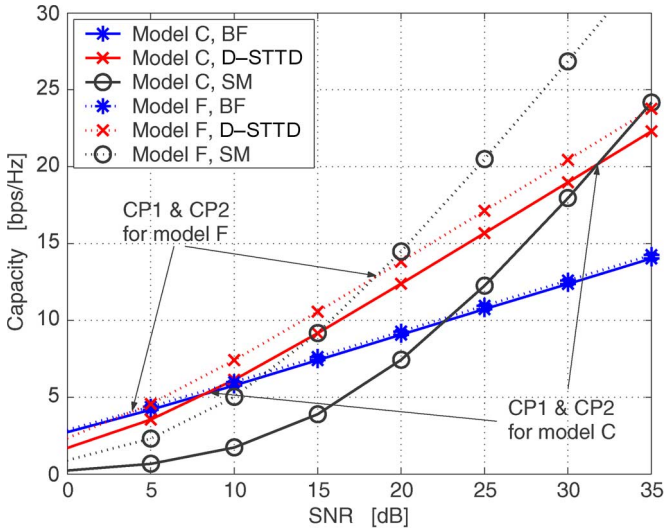


Fig. 4. Mean capacity for BF, D-STTD (with ZF), SM (with ZF) in the IEEE 802.11n channel models C and F (NLOS). CP1: crossing-point BF versus D-STTD; CP2: crossing-point D-STTD versus SM.

large SNR between the SM and optimal capacity curves could be reduced by employing other higher complexity receivers than linear receivers, such as successive interference cancellation (SIC). For our practical adaptive algorithm presented in Section V, however, we consider low-complexity codes for which linear receivers are preferable over SIC receivers (for more details, see [32]).

These results demonstrate that there are significant capacity benefits to be gained (over fixed transmission) by adaptively switching between the low-complexity transmission schemes we are considering, based on the operating SNR. As seen from the figure, such an adaptive scheme would perform closer to the optimal curve for all SNRs. Note, however, that although optimal transmission still yields a noticeable capacity advantage at many SNRs, this transmission approach is not suitable for practical MIMO systems due to the high computational complexity involved in solving the optimization problem (7). On the other hand, our low-complexity adaptive MIMO approach is particularly suited to practical systems.

Fig. 4 shows capacity curves for the same low-complexity transmission schemes as in Fig. 3, comparing different channel correlation scenarios. In particular, IEEE 802.11a models C and F [12] are considered, where model C is characterized by a lower angle spread and a smaller number of scatterer clusters than model F, resulting in higher levels of spatial correlation. We see that the relative capacity performance of the transmission schemes varies significantly, depending on the channel correlation scenario. Specifically, for model C, the crossing points of the BF/D-STTD and D-STTD/SM capacity curves (marked on the figure as CP1 and CP2, respectively) occur at SNRs thresholds of 8.2 and 31.8 dB, respectively. For model F, these thresholds occur at the much lower SNRs of 3.7 and 18.4 dB, respectively. These results suggest that a practical switching algorithm for the proposed low-complexity adaptive MIMO approach (i.e., based on BF, D-STTD, and SM) should be designed to exploit both the average SNR and channel spatial correlation information.

In the following section, we gain further insights into the key parameters affecting the relative capacity performance, by deriving closed-form theoretical expressions for the capacity crossing-points in some representative scenarios, for the case of BF and SM transmission.

### *B. Theoretical Crossing-Points Between BF and SM Capacity Curves*

Our crossing-point investigation is based on the tight upper bounds (27) and (38), for BF and SM transmission, respectively. To derive the theoretical crossing points, it is useful to manipulate the SM capacity (38) into a slightly different form. We start by writing

$$C_{\mathrm{SM}} \leq \log_2\left(\prod_{k=1}^{N_{\mathrm{t}}}\left(1+\frac{(N_{\mathrm{r}}-N_{\mathrm{t}}+1)|\mathbf{S}|\gamma_{\mathrm{o}}}{N_{\mathrm{t}}|\mathbf{S}^{kk}|}\right)\right) = \log_2\left|\mathbf{I}_{N_{\mathrm{t}}}+\mathrm{diag}\left(\frac{(N_{\mathrm{r}}-N_{\mathrm{t}}+1)|\mathbf{S}|\gamma_{\mathrm{o}}}{N_{\mathrm{t}}|\mathbf{S}^{kk}|}\right)\right|. \quad (44)$$

Now, using a determinant expansion from [33], we express the SM capacity as a polynomial in $\gamma_{\mathrm{o}}$ as follows:

$$\begin{aligned} C_{\mathrm{SM}} &\leq \log_2\left(1+\sum_{k=1}^{N_{\mathrm{t}}}\gamma_{\mathrm{o}}^k\left(\frac{N_{\mathrm{r}}-N_{\mathrm{t}}+1}{N_{\mathrm{t}}}\right)^k \mathrm{tr}_k \right. \\ &\qquad \left. \times\left(\mathrm{diag}\left(\frac{|\mathbf{S}|}{|\mathbf{S}^{11}|},\ldots,\frac{|\mathbf{S}|}{|\mathbf{S}^{N_{\mathrm{t}}N_{\mathrm{t}}}|}\right)\right)\right) \\ &= \log_2\left(1+\sum_{k=1}^{N_{\mathrm{t}}}\gamma_{\mathrm{o}}^k\left(\frac{N_{\mathrm{r}}-N_{\mathrm{t}}+1}{N_{\mathrm{t}}}|\mathbf{S}|\right)^k \mathrm{tr}_k(\mathbf{A})\right) \end{aligned} \quad (45)$$

where

$$\mathbf{A} = \mathrm{diag}\left(\frac{1}{|\mathbf{S}^{11}|},\ldots,\frac{1}{|\mathbf{S}^{N_{\mathrm{t}}N_{\mathrm{t}}}|}\right) \quad (46)$$

and where $\mathrm{tr}_k(\cdot)$ denotes the $k$th elementary symmetric function, which is defined as [28], [34]

$$\mathrm{tr}_k(\mathbf{X}) = \sum_{\{\underline{\alpha}\}}\prod_{i=1}^{k}\lambda_{x,\alpha_i} = \sum_{\{\underline{\alpha}\}}|\mathbf{X}_{\underline{\alpha}}^{\underline{\alpha}}| \quad (47)$$

for arbitrary Hermitian positive-definite $\mathbf{X}\in\mathbb{C}^{n\times n}$. In (47), the sum is over all ordered $\underline{\alpha}=\{\alpha_1,\ldots,\alpha_k\}\subseteq\{1,\ldots,n\}$, $\lambda_{x,i}$ denotes the $i$th eigenvalue of $\mathbf{X}$, and $\mathbf{X}_{\underline{\alpha}}^{\underline{\alpha}}$ is the $k\times k$ principle submatrix of $\mathbf{X}$ formed by taking only the rows and columns indexed by $\underline{\alpha}$.

Comparing (45) with the BF capacity bound in (27) we find that the SNR threshold $\gamma_{\mathrm{CP}}$ corresponding to the capacity crossing-point is given by the positive solution to the polynomial equation

$$\sum_{k=1}^{N_{\mathrm{t}}}\gamma_{\mathrm{CP}}^{k-1}\left(\frac{N_{\mathrm{r}}-N_{\mathrm{t}}+1}{N_{\mathrm{t}}}|\mathbf{S}|\right)^k \mathrm{tr}_k(\mathbf{A}) - N_{\mathrm{r}}\lambda_{\mathrm{s,max}} = 0. \quad (48)$$

We now present closed-form expressions for $\gamma_{\mathrm{CP}}$ for two special cases in order to gain further insight.

*1) Case:* $2 \times N_{\mathrm{r}}$*:* In this case, from (46) and (47), we have $\mathrm{tr}_1(\mathbf{A}) = 2$ and $\mathrm{tr}_2(\mathbf{A}) = 1$, and it is easily shown that the solution to (48) is given by

$$\gamma_{\mathrm{CP}} = \frac{4\left(N_{\mathrm{r}}\lambda_{s,\max} - (N_{\mathrm{r}}-1)|\mathbf{S}|\right)}{(N_{\mathrm{r}}-1)^2\,|\mathbf{S}|^2}. \tag{49}$$

This result shows that the SNR thresholds, defining the relative performance of the low-complexity transmission schemes, depend explicitly on the eigenvalues of the transmit correlation matrix (i.e., through the determinant). This information is exploited in our proposed practical switching algorithm, as detailed in the following section. It is also interesting to observe that the capacity crossing-point varies inversely to the number of receive antennas, indicating that the relative capacity improvement due to the increased receive diversity is greater for SM transmission than for BF.

For the special case $N_{\mathrm{r}} = 2$, the capacity crossing-point further simplifies as follows:

$$\gamma_{\mathrm{CP}} = \frac{4}{|\mathbf{S}|}\left(\frac{2}{\lambda_{s,\min}} - 1\right). \tag{50}$$

*2) Case:* $3 \times N_{\mathrm{r}}$*:* In this case, (48) reduces to a simple quadratic equation. Solving this, and simplifying using (46) and (47), we obtain

$$\gamma_{\mathrm{CP}} = \sqrt{\frac{\mathrm{tr}_2(\mathbf{A})^2 - 4|\mathbf{A}|\left(\mathrm{tr}(\mathbf{A}) - \frac{3\lambda_{s,\max}N_{\mathrm{r}}}{(N_{\mathrm{r}}-2)|\mathbf{S}|}\right) - \mathrm{tr}_2(\mathbf{A})}{\frac{2}{3}(N_{\mathrm{r}}-2)|\mathbf{A}||\mathbf{S}|}}. \tag{51}$$

For the special case $N_{\mathrm{r}} = 3$, this result further simplifies to

$$\gamma_{\mathrm{CP}} = \sqrt{\frac{\mathrm{tr}_2(\mathbf{A})^2 - 4|\mathbf{A}|\left(\mathrm{tr}(\mathbf{A}) - \frac{9\lambda_{s,\max}}{|\mathbf{S}|}\right) - \mathrm{tr}_2(\mathbf{A})}{\frac{2}{3}|\mathbf{A}||\mathbf{S}|}}. \tag{52}$$

Again, we see a dependence on the eigenvalues of the transmit spatial correlation matrix.

*3) Numerical Crossing-Point Results:* Fig. 5 shows the SNR threshold (49) as a function of the angular spread (AS), for $N_{\mathrm{t}} = 2$ and different numbers of receive antennas. The correlated MIMO channel is generated assuming a single scatterer cluster around the transmitter, with a broadside mean angle of departure (with respect to the antenna array).

We see that the SNR threshold varies inversely to the AS. This is due to the fact that increasing the AS reduces the level of spatial correlation (or equivalently, increases the spatial selectivity), in which case the maximum eigenvalue of the transmit correlation matrix $\lambda_{s,\max}$ also reduces, thereby decreasing $\gamma_{\mathrm{CP}}$ consistently with (49). The figure also shows that the SNR threshold becomes very large for AS below 10°, for all antenna configurations. This indicates that SM transmission is particularly sensitive to high levels of spatial correlation.

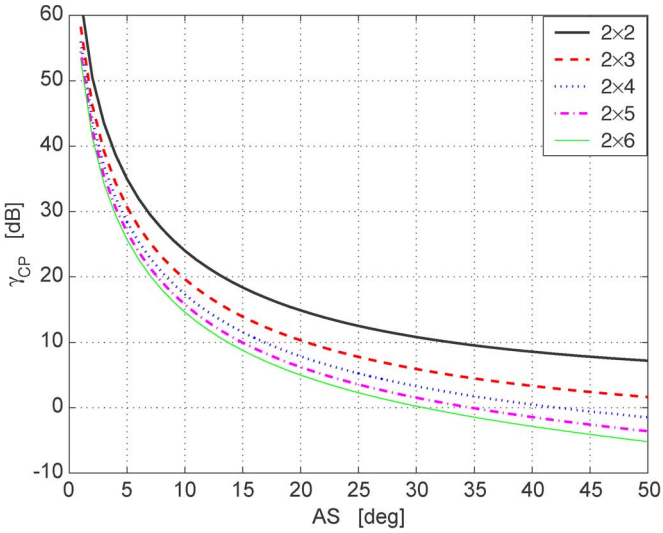


Fig. 5. Crossing-points for a MIMO $(N_{\mathrm{r}}, 2)$ system as a function of the AS and number of receive antennas $(N_{\mathrm{r}})$. Single-sided correlated channel with single cluster and mean angle of departure at 0° (broadside direction).

## V. Practical Adaptive MIMO Algorithm

In the preceding section, we demonstrated significant theoretical capacity gains offered by the proposed low-complexity adaptive MIMO approach and also identified the important factors from a switching point of view. We now propose a novel algorithm for switching between the low-complexity transmission schemes in a practical wireless communication system. The goal of our algorithm is to maximize the system spectral efficiency for a predefined target bit error rate (BER).

### A. MIMO Transmission Modes

Our adaptive switching algorithm operates according to a set of modes, with each mode comprising a particular low-complexity MIMO transmission technique and a modulation/coding scheme (MCS). The MIMO transmission schemes we consider include statistical BF, D-STTD with mmse receivers, and SM with mmse receivers. We consider the eight MCS combinations defined by the IEEE 802.11a standard [35]. The three MIMO transmission schemes and the eight MCS combinations yield a total of 24 different transmission modes, from which we select a subset of 12 (including a no transmission mode, for cases where the target error rate is not satisfied by any of the other selected modes).

### B. Link-Quality Regions and Metrics

Motivated by the results of Section IV, our proposed practical mode selection (or switching) algorithm is based on average SNR and channel correlation (eigenvalue) parameters. Unfortunately, defining switching criterion (i.e., a set of SNR switching thresholds, see below) for every channel correlation scenario is an infeasible solution. As such, our practical approach is to define a set of "typical" channel scenarios, and to precompute the error rate performance of the transmission modes for each

TABLE I
TYPICAL CHANNEL SCENARIOS USED BY OUR PRACTICAL ADAPTIVE SWITCHING ALGORITHM AND CORRESPONDING VALUES OF THE LINK-QUALITY METRIC ($D_\lambda$)

| Scenario | Channel Type | Spatial Parameters | $D_\lambda$ |
|---|---|---|---|
| 1 | NLOS, High AS | $K = -\infty$ dB, AS $\in [28^\circ, 55^\circ]$, $N_c = 6$ | [1,5.5) |
| 2 | NLOS, Low AS | $K = -\infty$ dB, AS $\in [22.4^\circ, 24.6^\circ]$, $N_c = 2$ | [5.5,25.8) |
| 3 | LOS, Low $K$ | $K = 2$ dB, AS $\in [22.4^\circ, 24.6^\circ]$, $N_c = 2$ | [25.8,85.8) |
| 4 | LOS, High $K$ | $K = 6$ dB, AS$= 30^\circ$, $N_c = 1$ | [85.8,+ inf) |

scenario. The typical channel scenarios we consider are detailed in Table I, with parameters $K$ and $N_c$ corresponding to the Rician $K$-factor in (2) and the number of scatterer clusters, respectively. These were selected based on the IEEE 802.11n models [12] and correspond to channels with widely varying degrees of spatial selectivity. For more details, see [10].

For each typical channel scenario we associate a corresponding set of SNR thresholds, which together define the link-quality regions used for mode selection. To predict the link-quality region for a given transmission we employ two link-quality metrics: the average SNR, and the relative condition number ($D_\lambda$) of the spatial correlation matrices. The relative condition number is a function of the eigenvalues of the spatial correlation matrices, as discussed in [10], and is an indicator of the channel spatial-selectivity.

### C. Generating the Lookup Table (LUT)

The mode selection information, corresponding to the set of link quality regions, is stored in a LUT. To generate the LUT, we simulate the error-rate performance of the 24 transmission modes in the four typical channels scenarios, and in each case determine the SNR thresholds corresponding to a predefined target error rate. For each channel scenario, we then select a subset of the 12 modes providing increasing transmission rates with the lowest SNR thresholds. The SNR thresholds corresponding to the selected modes for each channel scenario are then stored in the LUT.

### D. Switching Algorithm Operation

Once the LUT is constructed, our proposed practical switching algorithm operates as follows. The receiver first calculates the link quality metrics by measuring the average SNR and the relative condition number ($D_\lambda$) of the channel spatial correlation matrices. These metrics are then input into the LUT, which maps the link-quality metrics into a link-quality region. In particular, $D_\lambda$ is used to select the channel scenario, according to the empirically derived values reported in Table I. Then, the average SNR is compared against the SNR thresholds of the selected channel scenario to choose the optimal transmission mode, providing the highest throughput for the predefined target error rate. The mode-selection information is then conveyed to the transmitter via a reliable low-rate feedback channel.

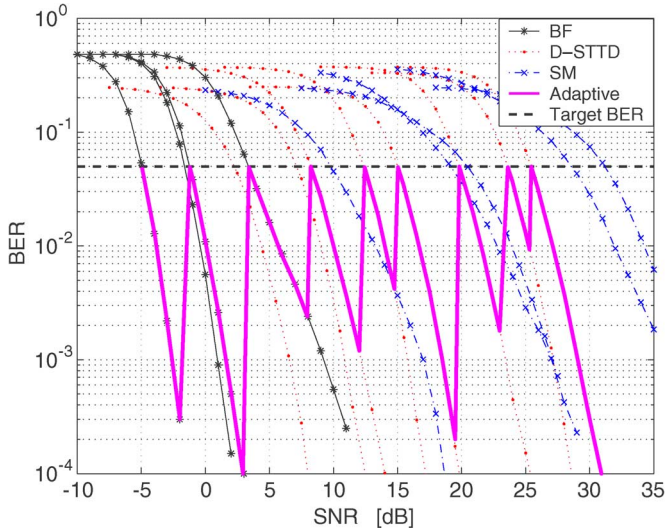


Fig. 6. BER of the adaptive MIMO transmission scheme versus fixed BF, D-STTD, and SM with different MCS, in channel scenario 4.

Note that the switching criterion is derived from the channel statistics (i.e., average SNR and spatial correlation) rather than instantaneous channel state information. As such, the proposed method tracks the long-term channel variations (due to shadowing, path-loss, or different correlation scenarios), thereby reducing the amount of feedback required for the adaptive mode switching. Also, since it is based on statistical knowledge, the algorithm is inherently more robust to practical effects such as imperfect channel estimation and feedback delays.

### E. Simulation Results

For the following simulation results, we assume a $4 \times 4$ MIMO system and a target BER of 0.05. Fig. 6 shows the BER versus SNR curves for each of the transmission modes for typical channel scenario 4 in Table I. The BER performance of the adaptive scheme is shown by the thicker solid line. As the SNR is increased, modes with increasing levels of spectral efficiency are selected. We clearly see that in all cases the BER of

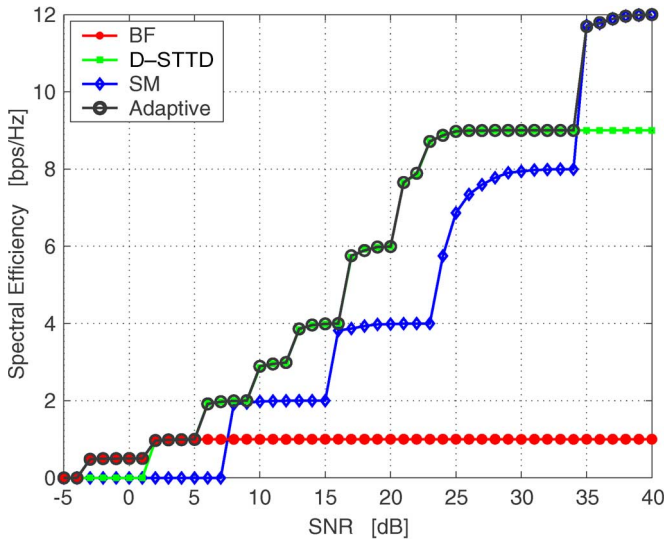


Fig. 7. Spectral efficiency of the adaptive MIMO transmission scheme versus fixed BF, D-STTD, and SM with adaptive MCS, in channel scenario 3 in [10].

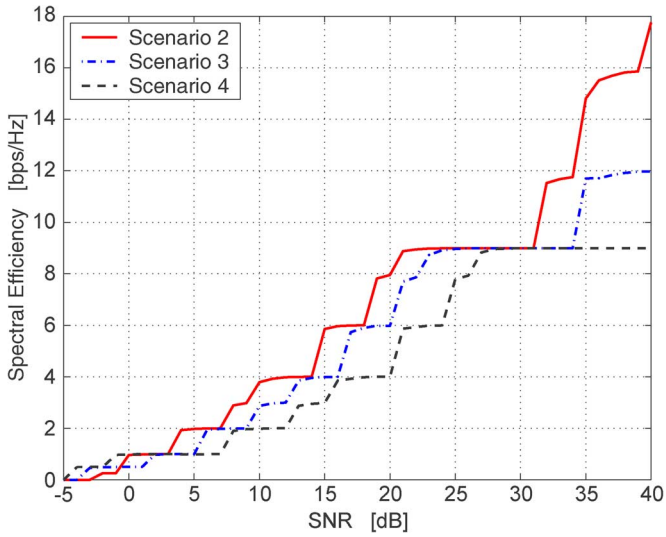


Fig. 8. Spectral efficiency of the adaptive MIMO transmission scheme in different channel scenarios.

the adaptive scheme remains below the predefined target, as required.

Fig. 7 compares the spectral efficiency of the proposed adaptive algorithm, with that of fixed BF, D-STTD, and SM transmission schemes employing adaptive MCS. Results are presented in typical channel scenarios 3, as defined in Table I. We see that, for high SNR, the proposed adaptive algorithm yields a spectral efficiency gain of 11 b/s/Hz over a non-adaptive BF scheme. We emphasize that the BER for the adaptive scheme remains below the predefined target for all levels of spectral efficiency. Note that the low performance of statistical BF in this case is due to the presence of multiple clusters for channel scenario 3, which prevents the channel from having one dominant spatial direction in narrowband systems. In broadband systems, where multiple taps are distinguishable both in time and space, better performance is expected for BF.

Fig. 8 depicts the spectral efficiency curves for the adaptive algorithm in different channel scenarios. It is possible to see that in a low-SNR regime, the spectral efficiency improves from scenario 2 to 4 in Table I due to the increasing channel spatial correlation that yields better performance for BF. Vice versa, for SNR higher than 5 dB, the throughput provided by the adaptive algorithm tends to decrease from scenario 2 to 4, since the performance of D-STTD and SM degenerates as the spatial correlation increases.

## VI. Conclusion

We presented a low-complexity adaptive MIMO transmission approach for spatially correlated channels. Based on new theoretical capacity expressions for BF, SM and D-STTD, we showed that the proposed adaptive system offered substantial capacity improvements over nonadaptive transmission and approached the optimal capacity in various scenarios. We also derived expressions for the optimal SNR switching thresholds and identified key switching parameters used to define switching criteria for our practical switching algorithm. Finally, we showed that our practical switching algorithm yields significant gain in spectral efficiency and improved error rate performance over nonadaptive schemes.

## Appendix

Using $\mathcal{H}$ in (39), we define

$$\mathbf{C} \triangleq \mathcal{H}^{\dagger}\mathcal{H} = \begin{bmatrix} c_1 & 0 & c_3 & c_4 \\ 0 & c_1 & -c_4^* & c_3^* \\ c_3^* & -c_4 & c_2 & 0 \\ c_4^* & c_3 & 0 & c_2 \end{bmatrix} \tag{53}$$

where

$$\begin{aligned} c_1 &= \sum_{m=1}^{N_r} \left(|h_{m,1}|^2 + |h_{m,2}|^2\right) \\ c_2 &= \sum_{m=1}^{N_r} \left(|h_{m,3}|^2 + |h_{m,4}|^2\right) \qquad (54) \\ c_3 &= \sum_{m=1}^{N_r} \left(h_{m,1}^* h_{m,3} + h_{m,2} h_{m,4}^*\right) \\ c_4 &= \sum_{m=1}^{N_r} \left(-h_{m,1}^* h_{m,4} + h_{m,2} h_{m,3}^*\right). \qquad (55) \end{aligned}$$

We now show that the first two diagonal entries of $\mathbf{C}^{-1}$ are equal to each other, and so are the last two diagonal entries. This in turn would mean that in (31), we have $\gamma_1 = \gamma_2$ and $\gamma_3 = \gamma_4$.

Note that $\mathbf{C}$ in (53) can be written in a partitioned form as

$$\mathbf{C} = \begin{bmatrix} c_1\mathbf{I} & \mathbf{B} \\ \mathbf{B}^{\dagger} & c_2\mathbf{I} \end{bmatrix} \tag{56}$$

with

$$\mathbf{B} \triangleq \begin{bmatrix} c_3 & c_4 \\ -c_4^* & c_3^* \end{bmatrix}. \tag{57}$$

Observe that the matrix $\mathbf{B}$ is orthonormal and that

$$\mathbf{B}\mathbf{B}^\dagger = \{|c_3|^2 + |c_4|^2\}\mathbf{I} = \mathbf{B}^\dagger\mathbf{B}. \tag{58}$$

The inverse of $\mathbf{C}$ clearly exists and, using the formula for the inverse of partitioned matrices [28], is given by

$$\mathbf{C}^{-1} = \begin{bmatrix} \left(c_1\mathbf{I} - \frac{1}{c_2}\mathbf{B}\mathbf{B}^\dagger\right)^{-1} & \frac{1}{c_1}\mathbf{B}\left(\frac{1}{c_1}\mathbf{B}^\dagger\mathbf{B} - c_2\mathbf{I}\right)^{-1} \\ \frac{1}{c_1}\left(\frac{1}{c_1}\mathbf{B}^\dagger\mathbf{B} - c_2\mathbf{I}\right)^{-1}\mathbf{B}^\dagger & \left(c_2\mathbf{I} - \frac{1}{c_1}\mathbf{B}^\dagger\mathbf{B}\right)^{-1} \end{bmatrix} \tag{59}$$

$$= \begin{bmatrix} \left(c_1 - \frac{(|c_3|^2+|c_4|^2)}{c_2}\right)^{-1}\mathbf{I} & \frac{1}{c_1}\left(\frac{(|c_3|^2+|c_4|^2)}{c_1} - c_2\right)^{-1}\mathbf{B} \\ \frac{1}{c_1}\left(\frac{(|c_3|^2+|c_4|^2)}{c_1} - c_2\right)^{-1}\mathbf{B}^\dagger & \left(c_2 - \frac{(|c_3|^2+|c_4|^2)}{c_1}\right)^{-1}\mathbf{I} \end{bmatrix}. \tag{60}$$

Substituting (60) into (31), it is easy to see that $\gamma_1 = \gamma_2$, $\gamma_3 = \gamma_4$ and that the random variables $\gamma_k$ (with $k = 1, \ldots, 4$) are identically distributed. The same results hold even in the case of (30). To see this, define $\tilde{\mathbf{C}} = \mathbf{I}_{N_\mathrm{t}} + (\gamma_\mathrm{o}/N_\mathrm{t})\mathbf{C}$ and note that $\tilde{\mathbf{C}}$ can be written in a partitioned matrix form similar to (56), with the corresponding submatrix of $\tilde{\mathbf{C}}$ obeying analogous relations (57) and (58). Hence, the elements of $\tilde{\mathbf{C}}^{-1}$ will also be such that the first two diagonal elements equal each other, and so do the last two diagonal elements.

## REFERENCES


[1] A. Paulraj, R. Nabar, and D. Gore, *Introduction to Space-Time Wireless Communications*. New York: Cambridge Univ. Press, 2003.

[2] L. Zheng and D. N. C. Tse, "Diversity and multiplexing: A fundamental tradeoff in multiple-antenna channels," *IEEE Trans. Inf. Theory*, vol. 49, no. 5, pp. 1073–1096, May 2003.

[3] R. W. Heath, Jr. and A. Paulraj, "Switching between multiplexing and diversity based on constellation distance," in *Proc. Allerton Conf. Commun. Control and Comput.*, Sep. 2000, pp. 212–221.

[4] S. Catreux, V. Erceg, D. Gesbert, and R. W. Heath, Jr., "Adaptive modulation and MIMO coding for broadband wireless data networks," *IEEE Commun. Mag.*, vol. 2, no. 6, pp. 108–115, Jun. 2002.

[5] G. D. Durgin, *Space-Time Wireless Channels*. Upper Saddle River, NJ: Prentice-Hall, 2003.

[6] D.-S. Shiu, G. J. Foschini, M. J. Gans, and J. M. Kahn, "Fading correlation and its effect on the capacity of multielement antenna systems," *IEEE Trans. Commun.*, vol. 48, no. 3, pp. 502–513, Mar. 2000.

[7] A. Forenza and R. W. Heath, Jr., "Impact of antenna geometry on MIMO communication in indoor clustered channels," in *Proc. IEEE Antennas and Propag. Symp.*, Jun. 2004, vol. 2, pp. 1700–1703.

[8] M. Bengtsson, D. Astely, and B. Ottersten, "Measurements of spatial characteristics and polarization with a dual polarized antenna array," in *Proc. IEEE Veh. Technol. Conf.*, vol. 1, May 1999, pp. 366–370.

[9] H. Bölcskei, M. Borgmann, and A. J. Paulraj, "Impact of the propagation environment on the performance of space-frequency coded MIMO-OFDM," *IEEE J. Sel. Areas Commun.*, vol. 21, no. 3, pp. 427–439, Apr. 2003.

[10] A. Forenza, A. Pandharipande, H. Kim, and R. W. Heath, Jr., "Adaptive MIMO transmission scheme: Exploiting the spatial selectivity of wireless channels," in *Proc. IEEE Veh. Technol. Conf.*, May 2005, vol. 5, pp. 3188–3192.

[11] A. Forenza, M. R. McKay, A. Pandharipande, R. W. Heath, Jr., and I. B. Collings, "Capacity enhancement via multi-mode adaptation in spatially correlated MIMO channels," in *Proc. IEEE Int. Symp. Pers., Indoor and Mobile Radio Commun.*, Sep. 2005, pp. 754–758.

[12] V. Erceg *et al.*, *TGn Channel Models*, IEEE 802.11-03/940r4, May 2004.

[13] E. A. Jorswieck and H. Boche, "Channel capacity and capacity-range of beamforming in MIMO wireless systems under correlated fading with covariance feedback," *IEEE Trans. Wireless Commun.*, vol. 3, no. 5, pp. 1543–1553, Sep. 2004.

[14] A. L. Moustakas and S. H. Simon, "Optimizing multiple-input single-output (MISO) communication systems with general Gaussian channels: Nontrivial covariance and nonzero mean," *IEEE Trans. Inf. Theory*, vol. 49, no. 10, pp. 2770–2780, Oct. 2003.

[15] M. Kang and M. S. Alouini, "Water-filling capacity and beamforming performance of MIMO systems with covariance feedback," in *Proc. IEEE Workshop Signal Process. Adv. Wireless Commun.*, Jun. 2003, pp. 556–560.

[16] S. H. Simon and A. L. Moustakas, "Optimizing MIMO antenna systems with channel covariance feedback," *IEEE J. Sel. Areas Commun.*, vol. 21, no. 3, pp. 406–417, Apr. 2003.

[17] S. A. Jafar, S. Vishwanath, and A. Goldsmith, "Channel capacity and beamforming for multiple transmit and receive antennas with covariance feedback," in *Proc. IEEE Int. Conf. Commun.*, Jun. 2001, vol. 7, pp. 2266–2270.

[18] A. M. Mathai and S. B. Provost, *Quadratic Forms in Random Variables*. New York: Marcel Dekker, 1992.

[19] I. S. Gradshteyn and I. M. Ryzhik, *Table of Integrals, Series, and Products*, 1st ed. New York: Academic, 1994.

[20] P. J. Smith, S. Roy, and M. Shafi, "Capacity of MIMO systems with semicorrelated flat fading," *IEEE Trans. Inf. Theory*, vol. 49, no. 10, pp. 2781–2788, Oct. 2003.

[21] M. Chiani, M. Z. Win, and A. Zanella, "On the capacity of spatially correlated MIMO Rayleigh-fading channels," *IEEE Trans. Inf. Theory*, vol. 49, no. 10, pp. 2363–2371, Oct. 2003.

[22] M. Kiessling and J. Speidel, "Mutual information of MIMO channels in correlated Rayleigh fading environments—A general solution," in *Proc. IEEE Int. Conf. Commun.*, Jun. 2004, vol. 2, pp. 814–818.

[23] M. R. McKay and I. B. Collings, "General capacity bounds for spatially correlated Rician MIMO channels," *IEEE Trans. Inf. Theory*, vol. 51, no. 9, pp. 3121–3145, Sep. 2005.

[24] ——, "Capacity bounds for correlated Rician MIMO channels," in *Proc. Int. Conf. Commun.*, 2005, pp. 772–776.

[25] M. Kiessling and J. Speidel, "Ergodic capacity of MIMO channels with statistical channel state information at the transmitter," in *Proc. ITG Workshop Smart Antennas*, Mar. 2004, pp. 79–86.

[26] D. Gore, R. W. Heath, and A. Paulraj, "Transmit selection in spatial multiplexing systems," *IEEE Commun. Lett.*, vol. 6, no. 11, pp. 491–493, Nov. 2002.

[27] R. W. Heath, S. Sandhu, and A. Paulraj, "Antenna selection for spatial multiplexing systems with linear receivers," *IEEE Commun. Lett.*, vol. 5, no. 4, pp. 142–144, Apr. 2001.

[28] R. A. Horn and C. R. Johnson, *Matrix Analysis*, 4th ed. New York: Cambridge Univ. Press, 1990.

[29] E. N. Onggosanusi, A. G. Dabak, and T. A. Schmidl, "High rate space-time block coded scheme: Performance and improvement in correlated fading channels," in *Proc. IEEE Wireless Commun. and Netw. Conf.*, Mar. 2002, vol. 1, pp. 194–199.

[30] B. Hassibi and B. M. Hochwald, "High-rate codes that are linear in space and time," *IEEE Trans. Inf. Theory*, vol. 48, no. 7, pp. 1804–1824, Jul. 2002.

[31] T. Takahama and S. Sakai, "Constraint optimization by $\alpha$ constraint genetic algorithm ($\alpha$GA)," *Syst. Comput. Jpn.*, vol. 35, no. 5, pp. 11–22, May 2004.

[32] K. B. Song, "Value of adaptive transmission and effect of imperfect decision feedback in practical wireless systems," Ph.D. dissertation, Stanford Univ., Stanford, CA, 2005.

[33] A. C. Aitken, *Determinants and Matrices*, 9th ed. Edinburgh, U.K.: Oliver & Boyd, 1956.

[34] A. W. Marshall and I. Olkin, *Inequalities: Theory of Majorization and Its Applications*. New York: Academic, 1979.

[35] *Part 11: Wireless LAN Medium Access Control (MAC) and Physical Layer (PHY) Specifications: High-Speed Physical Layer in the 5 GHz Band*, IEEE Stand. 802.11a, 1999.

**Antonio Forenza** (S'04-M'06) received the M.S. degree in telecommunications engineering from Politecnico di Torino, Torino, Italy, and Eurecom Institute, Sophia Antipolis, France, in 2001 and the Ph.D. degree in electrical and computer engineering from the University of Texas at Austin in 2006.

In 2001, he interned as a Systems Engineer at Iospan Wireless, Inc., San Jose, CA, which is a startup company that developed the first commercial MIMO-OFDM communication system. His main research focus was on link-adaptation and physical layer algorithm design. In the fall of 2001, he joined ArrayComm, Inc., San Jose, as a Systems Research Engineer. At ArrayComm, he was actively involved in the design and implementation of smart antenna systems for the 3G WCDMA wireless platform. Over the summers of 2004 and 2005, he interned as a Research Engineer at Samsung Advanced Institute of Technology, Suwon, Korea, and Freescale Semiconductor, Inc., Austin, respectively, developing adaptive MIMO transmission and multiuser MIMO precoding techniques for 3GPP, IEEE 802.11n, and IEEE 802.16e standards systems. Since June 2006, he has been with Rearden, LLC, San Francisco, CA, as a Senior Systems Engineer. His research interests include MIMO antenna design, adaptive MIMO transmission techniques, precoding methods for multiuser MIMO, and smart antenna signal processing.

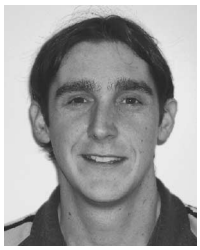

**Matthew R. McKay** (S'02) was born in Meningie, Australia, in 1979. He received the combined B.E. degree in electrical engineering and B.IT. degree in computer science from Queensland University of Technology, Brisbane, Australia, in 2002. He is currently working toward the Ph.D. degree in electrical engineering at University of Sydney, Sydney, Australia.

His current research interests include MIMO-OFDM, bit-interleaved coded modulation, information theory, and multivariate statistical theory.

Mr. McKay received the University Medal from Queensland University of Technology upon graduating in 2002. His research is supported by Australia's Commonwealth Scientific and Industrial Research Organisation (CSIRO), where he received a Postgraduate scholarship.

**Ashish Pandharipande** (S'97–A'98–M'03) received the B.E. degree in electronics and communications engineering from Osmania University, Hyderabad, India, in 1998 and the M.S. degrees in electrical and computer engineering and mathematics and the Ph.D. degree in electrical and computer engineering from the University of Iowa, Iowa City, in 2000, 2001, and 2002, respectively.

He was a Postdoctoral Researcher at the University of Florida, Gainesville, and then Senior Researcher at Samsung Advanced Institute of Technology, Suwon, Korea. He has held visiting positions at AT&T Laboratories, NJ, and the Department of Electrical Communication Engineering, Indian Institute of Science, Bangalore, India. He is currently a Senior Scientist at Philips Research, Eindhoven, The Netherlands. His research interests are in the areas of multicarrier and MIMO wireless communications, cognitive wireless systems, and multirate signal processing.

**Robert W. Heath Jr.** (S'96–M'01–SM'06) received the B.S. and M.S. degrees, both from University of Virginia, Charlottesville, in 1996 and 1997, respectively, and the Ph.D. degree from Stanford University, Stanford, CA, in 2002, all in electrical engineering.

From 1998 to 2001, he was a Senior Member of the Technical Staff then a Senior Consultant with Iospan Wireless, Inc., San Jose, CA, where he worked on the design and implementation of the physical and link layers of the first commercial MIMO-OFDM communication system. In 2003, he founded MIMO Wireless, Inc., which is a consulting company dedicated to the advancement of MIMO technology. Since January 2002, he has been with the Department of Electrical and Computer Engineering at The University of Texas at Austin, where he is currently an Assistant Professor and member of the Wireless Networking and Communications Group. His research interests cover a broad range of MIMO communication, including antenna design, practical receiver architectures, limited feedback techniques, *ad hoc* networking, and scheduling algorithms, as well as 60-GHz communication techniques.

Dr. Heath serves as an Editor for the IEEE TRANSACTIONS ON COMMUNICATION, an Associate Editor for the IEEE TRANSACTIONS ON VEHICULAR TECHNOLOGY, and is a member of the Signal Processing for Communications Technical Committee of the IEEE Signal Processing Society.

**Iain B. Collings** (S'92–M'95–SM'02) was born in Melbourne, Australia, in 1970. He received the B.E. degree in electrical and electronic engineering from University of Melbourne, Parkville, Australia, in 1992 and the Ph.D. degree in systems engineering from Australian National University, Canberra, Australia, in 1995.

Currently, he is a Science Leader with the Wireless Technologies Laboratory at CSIRO ICT Centre, Australia. Prior to this, he was an Associate Professor at the University of Sydney (1999–2005); a Lecturer at the University of Melbourne (1996–1999); and a Research Fellow in the Australian Cooperative Research Centre for Sensor Signal and Information Processing (1995). His current research interests include mobile digital communications and broadband digital subscriber line communications, more specifically, channel estimation, equalization, and multicarrier modulation, for time-varying, multiuser, and MIMO channels.

Dr. Collings currently serves as an Editor for the IEEE TRANSACTIONS ON WIRELESS COMMUNICATIONS and as a Guest Editor for the *EURASIP Journal on Advanced Signal Processing*. He has also served as the Vice Chair of the Technical Program Committee for IEEE Vehicular Technology Conference (Spring) 2006, as well as serving on a number of other TPC and organizing committees of IEEE conferences. He is also a Founding Organizer of the Australian Communication Theory Workshops 2000–2006.